Available online at www.sciencedirect.com
ScienceDirect
Biochimica et Biophysica Acta 1768 (2007) 1758–1768
Biochimica et Biophysica Acta
BBA
www.elsevier.com/locate/bbamem

Molecular organization of surfactin–phospholipid monolayers: Effect of phospholipid chain length and polar head

O. Bouffioux [a,1], A. Berquand [c,1], M. Eeman [b,1], M. Paquot [b], Y.F. Dufrêne [c], R. Brasseur [a], M. Deleu [b,*]

[a] Centre de Biophysique Moléculaire Numérique, Faculté Universitaire des Sciences Agronomiques de Gembloux, Passage des Déportés, 2, B-5030 Gembloux, Belgium
[b] Unité de Chimie Biologique Industrielle, Faculté Universitaire des Sciences Agronomiques de Gembloux, Passage des Déportés, 2, B-5030 Gembloux, Belgium
[c] Unité de Chimie des Interfaces, Université Catholique de Louvain, Croix du Sud 2/18, B-1348 Louvain-la-Neuve, Belgium

Received 9 November 2006; received in revised form 19 April 2007; accepted 20 April 2007
Available online 29 April 2007

Abstract

Mixed monolayers of the surface-active lipopeptide surfactin-C_{15} and various lipids differing by their chain length (DMPC, DPPC, DSPC) and polar headgroup (DPPC, DPPE, DPPS) were investigated by atomic force microscopy (AFM) in combination with molecular modeling (Hypermatrix procedure) and surface pressure-area isotherms. In the presence of surfactin, AFM topographic images showed phase separation for each surfactin–phospholipid system except for surfactin–DMPC, which was in good agreement with compression isotherms. On the basis of domain shape and line tension theory, we conclude that the miscibility between surfactin and phospholipids is higher for shorter chain lengths (DMPC > DPPC > DSPC) and that the polar headgroup of phospholipids influences the miscibility of surfactin in the order DPPC > DPPE > DPPS. Molecular modeling data show that mixing surfactin and DPPC has a destabilizing effect on DPPC monolayer while it has a stabilizing effect towards DPPE and DPPS molecular interactions. Our results provide valuable information on the activity mechanism of surfactin and may be useful for the design of surfactin delivery systems.

Keywords: Langmuir film; Atomic force microscopy; Molecular modeling; Miscibility; Stabilizing effect; Nanoscale resolution

1. Introduction

Surfactin (Fig. 1A) is a lipopeptide produced by various *Bacillus subtilis* strains. It is composed of a heptapeptide cycle (*L*-Glu–*L*-Leu–*D*-Leu–*L*-Val–*L*-Asp–*D*-Leu–*L*-Leu) closed by C_{13}–C_{15} hydroxy fatty acid forming a lactone ring system. Surfactin exhibits strong surface activity and important biological properties [1–7]. The interactions of surfactin with biological membranes are known to determine its biological activity and involve insertion into lipid bilayers, modification of membrane permeability by channels formation or by carrying mono- and divalent cations, and membrane solubilization by a detergent-like mechanism [8,9].

As the activity of surfactin occurs within the bilayer, it is interesting to investigate the behaviour of surfactin inside the lipid matrix, after its penetration process. Previous interfacial properties measurements and molecular modeling have provided valuable insight into the miscibility and molecular orientation of mixed surfactin-dipalmitoylphosphatidylcholine (DPPC) monolayers [10,11]. As known, lipid fraction of biological membranes is mainly composed of phospholipids varying by their chain length and their ionic character, which might have an influence on surfactin activity.

Two former studies have already been devoted to the lipid specificity of the interaction of surfactin with biological membrane models [9,12]. Although they give valuable information, contradictions between the two papers exist, and

* Corresponding author. Tel.: +32 81 62 22 32; fax: +32 81 62 22 31.
E-mail address: deleu.m@fsagx.ac.be (M. Deleu).
[1] These authors contributed equally to this work.

0005-2736/$ – see front matter © 2007 Elsevier B.V. All rights reserved.
doi:10.1016/j.bbamem.2007.04.015

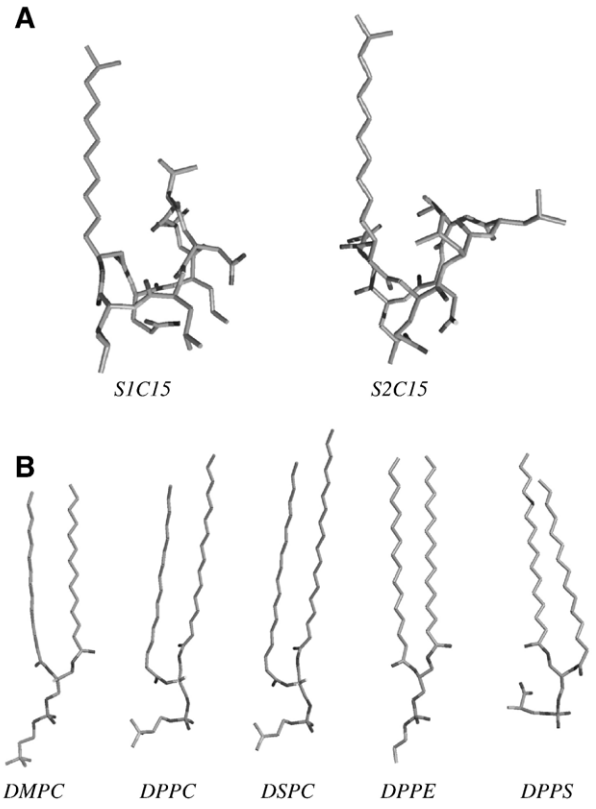

Fig. 1. Molecular models used in the multimolecular assemblies. (A) surfactin models; (B) phospholipid models.

particularly concerning the effect of surfactin on the interfacial organization of phospholipids. In the case of mixed monolayers of surfactin and dimyristoylphosphatidylcholine (DMPC), Maget-Dana and Ptak conclude that the two interfacial components are ideally miscible [9]. In other words, surfactin and DMPC do not specifically interact with each other and do not form a molecular complex. In contrast to their work, Grau et al. report the presence of specific molecular interactions between the DMPC acyl chains and the lipopeptide by performing differential scanning calorimetry on mixed surfactin–DMPC vesicles prepared in physiological conditions [12]. Such interactions are responsible of lateral phase separation of surfactin-rich domains within the bilayer. According to them, the domains are formed by clusters of surfactin and DMPC with a defined stoichiometry. Strong interaction between surfactin molecules is assumed to be at the origin of the phenomena. From their data, they did not see any pronounced difference between surfactin effects on DPPC and distearoylphosphatidylcholine (DSPC).

These two studies required further experimental data in order to reveal the presence or the absence of molecular interactions between the different interfacial components and consequently, to clarify their mixing behaviour. In this context, we have recently probed the interfacial behaviour of phospholipid monolayers following penetration of surfactin by using atomic force microscopy (AFM) [13]. Indeed, the ability of AFM to image surfaces at a nanometer lateral scale resolution and Angstrom vertical resolution makes it the technique of choice to distinguish domains in phase-separated films [14,15]. The presence or absence of domains and their morphology provide valuable information about molecular packing and organization of the components at the interface as well as about their miscibility on basis of the line tension theory. In this previous study, we showed that under physiological conditions the penetration power of surfactin and the nanoscale organization of the interfacial components at high surface pressure are more sensitive to the lateral arrangement of the phospholipids than to their chain length. In that work, AFM imaging was performed after surfactin penetration without being able to control the amount of lipopeptide inserted in the phospholipid monolayers and the transfer surface pressure of the mixed monolayers. As these two parameters play an important role in the mixing behaviour of the interfacial components, we propose, in the present study, to probe by AFM the interfacial organization of premixed surfactin–phospholipid monolayers spread with a defined molar ratio and compressed at a defined surface pressure.

Besides AFM, the Langmuir trough technique is used in order to have additional information on the interfacial properties of the film (miscibility, complex formation, thermodynamic stability) [10,16–18] in our experimental conditions. A procedure of molecular modeling (Hypermatrix procedure) is also applied to visualize at an atomic level the effect of surfactin on the lipid organization and to calculate the interaction energy in order to quantify the relative affinities between molecules and the stabilization effect of surfactin [11,19,20].

In addition to the effect of the phospholipid chain length, we also analyzed the influence of the phospholipid polar head on the interfacial behaviour of surfactin. Grau et al. have shown by performing DSC and X-ray diffraction experiments that addition of surfactin to dielaidoylphosphatidylethanolamine (DEPE) tends to destabilize the H_{II} structure [12]. Although their results do not show it explicitly, they conclude that surfactin is able to stabilize the DEPE bilayer. In our study, the combination of the three mentioned techniques is also used to provide new insight about this hypothesis.

Phospholipids with three different chain lengths (DMPC, DPPC and DSPC) and three different headgroups (DPPC, dipalmitoylphosphatidylethanolamine (DPPE) and dipalmitoylphosphatidylserine (DPPS)) are used in the present study. DMPC, DPPC and DSPC have two saturated fatty acid chains with 14, 16 and 18 carbon atoms respectively. As opposed to the work of Maget-Dana and Ptak [9], we use physiological conditions (Tris 10 mM NaCl 150 mM, pH 7.2) in order to be closer to the actual biological systems. In these conditions, DPPE and DPPC are zwitterionic, the polar head of DPPE being smaller than the DPPC one, while DPPS has a net negative charge. Surfactin is partially protonated at physiological pH.

The physico-chemical discussion of our results gives rise to a better understanding of the interaction between surfactin and lipid membrane at a molecular level. Moreover, they give some insight into the molecular mechanisms leading to the biological activity of surfactin. Finally, the work gives a critical view of the

three techniques, which can be useful for other studies concerning peptide–membrane interactions.

2. Experimental procedures

2.1. Molecular modeling

2.1.1. Surfactin and phospholipid structures

The structures of two surfactin homologues (S1 and S2) excreted by *Bacillus subtilis* were obtained from a previous modeling study [21]. Briefly, the atomic coordinates of the surfactins S1 and S2 come from a previous paper [22] and the fatty acid chain (C_{15}) was added and submitted to a systematic optimization bearing on all torsion axis (Fig. 1A). The surfactin molecules were modeled with a neutral global charge since in our experimental conditions, the two negative charges borne by surfactin are essentially shielded by Na^+ cations. Modeling did not take into consideration structural changes of the peptide part. Indeed, we considered that they are not so important because of its cyclic structure which ensures a certain rigidity.

DPPC [23], DPPS and DPPE were modeled using the same procedure. These systematic geometric optimizations require important resources in terms of calculation and time. So, we used the acyl chain conformation of DPPC as a starting point to build the myristic (DMPC) and stearic (DSPC) series by simply removing and adding the required methyl groups respectively. These new models were submitted to a geometric optimization with Hyperchem v 5.0 (Hypercube Inc., Gainesville, FL) using the molecular mechanics technique in the MM+ force field (Fig. 1B). The preferred structures of lipids in a solid-like state at room temperature (like DPPC, DSPC and DPPS) correspond to those presented by Brasseur et al. [23] and are in perfect agreement with experimental structures obtained by neutron diffraction [24]. For phospholipids in a fluid-like state in our conditions (like DMPC), the phosphate headgroup is more mobile and therefore adopts preferentially an extended structure. In the case of DPPE, it is well known that its bilayers form reversed hexagonal phase suggesting that PE headgroups are not very high hydrated. However, in a monolayer system, i.e. in the absence of an apposing membrane surface, a recent study [25] has shown by X-ray reflectivity experiments that the amine function in PE extends 1–2 Å further into the subphase than those of the PC headgroups. According to this study, not only is the exposure of the amine moiety to water in PE thus larger than that of the other lipids, but also the phosphate and lipid backbone of PE are more hydrated than that of PC. For this reason, we used in our modeling experiments an extended structure of the DPPE headgroup.

2.1.2. HYPERMATRIX procedure

The procedure to carry out an assembly of several surrounding molecules around a central molecule has been fully described previously [26]. Briefly, the central molecule is oriented according to the TAMMO procedure [27] allowing to take a hydrophobic/hydrophilic interface into account to orient the molecule according to its amphiphilicity. Then, the central molecule position was fixed and the surrounding molecule position was moved + and −10 Å along the x-axis by step of 0.2 Å (i.e. 100 times). For each x-axis position, the surrounding molecule was rotated by step of 15° around its long axis (24 times) and around the central molecule z-axis (24 times). The surrounding molecule was then moved + and −1.5 Å by step of 0.1 Å (i.e. 30 times) along the z-axis perpendicular to the interface. Finally, the tilt of the surrounding molecule was varied around the z-axis (+ and −10°) by step of 1° (i.e. 20 times). The energy of all possible positions (34.560×10^6) is calculated and only the complex of minimum energy is kept. Then, the position of the first surrounding molecule was fixed and the addition of a second surrounding molecule was considered. The energies of interaction between all molecules of the complex are considered and minimized until the lowest energy structure is reached. The intermolecular energy of interaction in the complex is calculated as the sum of the following terms: (a) The London–Van der Waals energy of interaction between atoms associated to different molecules. Buckingham's pairwise atom–atom interaction function has been used:

$$E_{\mathrm{vdW}} = \sum [A_{ij}\exp(-B_{ij}r_{ij}) - C_{ij}r_{ij}^{-6}] \quad (1)$$

where i and j are atoms, r_{ij} are their distances, and A, B, and C are coefficients assigned to atom pairs. We used values of the coefficients reported by Brasseur and co-workers [28]. These values emerge in part as the solution of the Schroëdinger equation and in part as heuristic variables. The problem in this potential is that if the atoms were to approach less than about 1 Å from one another, the r^{-6} attractive term becomes dominant, causing the total energy of the molecule to collapse to negative infinity. This is why an energy (E_{vdW}) of 100 kcal/mol is substituted for distances (r_{ij}) below 1 Å. (b) The generalised Keesom–Van der Waals interaction or electrostatic interaction between atomic point charges:

$$E_{\mathrm{cb}} = 332\left(\sum_{ij} e_i e_j / r_{ij}\varepsilon_{ij}\right) \quad (2)$$

where e_i and e_j are expressed in electron charge units and r_{ij} is in Å. The values of the atomic point charges are similar to the values used for polypeptides. To simulate the electrostatic properties of the membrane interface, we have assumed a dielectric constant (ε_{ij}) equal to 3 in the hydrophobic core and 30 in the water phase. Between these two media, there is an interface where the dielectric constant increases linearly along the z-axis perpendicular to the interface. (c) The transfer energy of atoms or groups of atoms from a hydrophobic phase to a hydrophilic phase accounting for their hydrophobic/hydrophilic properties.

2.2. Langmuir trough technique

2.2.1. Materials

Surfactin with a β-hydroxy fatty acid chain of 15 carbon atoms (molecular weight, 1035) was used in this study. It was produced and purified as previously described [29]. Primary structure and purity of the C_{15}-surfactin (>95%) were ascertained by analytical RP-HPLC, amino acid analysis and Maldi-Tof mass spectrometry measurements (Ultraflex TOF, Bruckner, Karisruhe, Germany), as in the previous study [10]. Dimyristoylphosphatidylcholine (DMPC) dipalmitoylphosphatidylcholine (DPPC), distearoylphosphatidylcholine (DSPC), dipalmitoylphosphatidylethanolamine (DPPE) and dipalmitoylphosphatidylserine (DPPS) were purchased from Avanti Polar Lipids (Alabaster, USA).

2.2.2. Preparation of monolayers

Pure and mixed monolayers were prepared at 20 °C with an automated LB system (KSV minitrough, KSV instruments Ltd., Helsinki, Finland). Phospholipids and surfactin were dissolved at 1 mM in chloroform/methanol (2/1). Pure solutions and (0.1/0.9), (0.25/0.75) molar mixtures of surfactin and phospholipids were spread on a Tris/NaCl 10/150 mM (Millipore Co., Milford, MA) subphase adjusted at pH 7.2 with HCl. After evaporation of the solvent (15 min), monolayers were compressed at a rate of 10 mm/min.

For AFM analysis, Langmuir–Blodgett monolayers were deposited at a constant surface pressure of 20 mN/m, i.e. well below the collapse pressure, by raising vertically freshly cleaved mica sheets through the air–water interface at a rate of 10 mm/min. The transfer ratios were close to 1:1.

2.3. AFM imaging

AFM measurements were carried out at room temperature (about 23 °C) in contact mode using an optical detection system (Nanoscope III, Digital Instruments, Santa Barbara, CA). Topographic images (512 X 512 pixels) were taken in the constant-deflection mode using oxide-sharpened microfabricated Si_3N_4 cantilevers (Park Scientific Instruments, Mountain View, CA) with typical curvature radii of 20 nm and spring constant of 0.01 and 0.03 N/m, as specified by the manufacturer. Scan rate ranging from 3 to 5 Hz was used. The applied force was maintained as low as possible during the imaging. The step heights between domains were determined using the digital instrument section analysis software, avoiding shadowed areas due to flattening effects. Five measurements were taken on at least three different samples on four different areas on each sample. The percentages of the surface covered by the bright phases were calculated using the bearing analysis software, using at least three different samples on four different areas.

3. Results and discussion

3.1. Effect of phospholipid chain length

The compression isotherms of pure surfactin, DMPC, DPPC and DSPC monolayers and mixed monolayers of surfactin with DMPC, DPPC and DSPC at a surfactin molar fraction (X_s) of 0.1 and 0.25 are presented in Fig. 2. The mixed curves lie between the curves of the pure components. At 20 mN/m, the surface pressure used for the LB transfer, one molecule of DMPC, DPPC and DSPC occupies 59.5, 48.2 and 48.5 $Å^2$ respectively. At this surface pressure, DMPC is in a liquid-expanded state while DPPC and DSPC are in a solid-like state, in agreement with literature [30–33]. DPPC and DSPC molecules adopt thus a vertical orientation with tight packing while DMPC molecules are less ordered and less compacted. The more flexible organization of DMPC is also demonstrated by its higher compressibility (proportional to $dA/d\Pi$), as already evoked by other authors [33]. At 20 mN/m, surfactin has a molecular area of 150.9 $Å^2$/molecule. The monolayer is in a liquid-expanded state and is thus less rigid than phosphatidylcholines except DMPC. Areas of the mixed surfactin–DMPC, surfactin-DPPC and surfactin-DSPC films at 20 mN/m vary linearly with the composition of the monolayer (data not shown), i.e. follow the additivity rule. It means in a first approach that either the two components are ideally miscible or completely immiscible [16].

After transfer on a solid mica support, mixed surfactin–phospholipid monolayers were imaged using AFM (Fig. 3). Very different morphologies of domains are obtained depending on the PC chain length. As a control, LB transfer and AFM analysis of pure DPPC monolayers at a surface pressure close to 20 mN/m was performed in order to assess the presence of 2D domains in our conditions. The image (data not shown) exhibited almost homogeneous contrast, with only very small domains dispersed in a uniform matrix. They can be attributed to the coexistence of few remaining liquid-expanded domains dispersed into a condensed matrix. In each case, their size and their morphology are completely different from the ones of domains observed in mixed surfactin–

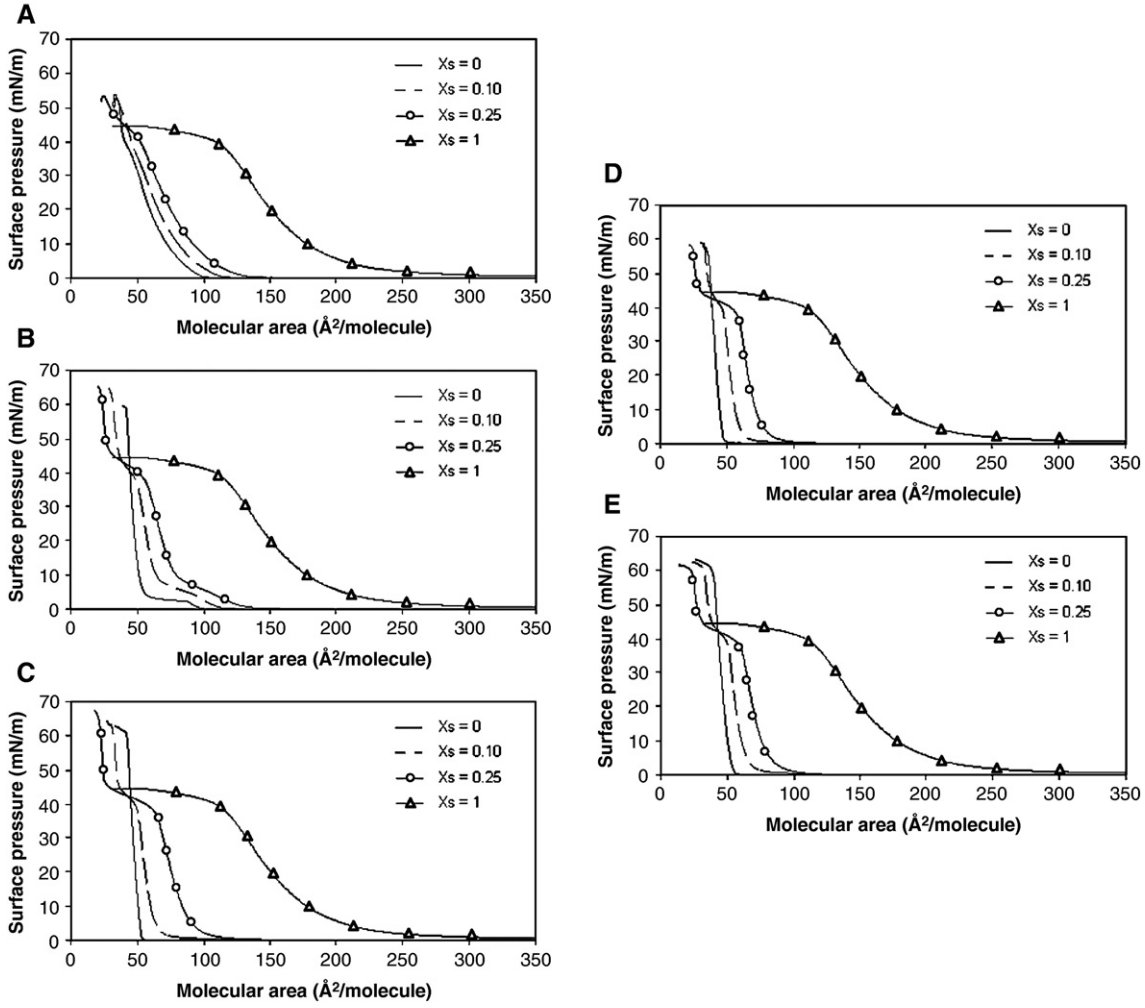

Fig. 2. Interfacial properties of mixed surfactin–phospholipid monolayers. Surface pressure-area (π-A) isotherms, at the air–water interface, of pure surfactin monolayer, pure phospholipid monolayer and mixed surfactin–phospholipid monolayers (A: DMPC; B: DPPC; C: DSPC; D: DPPE; E: DPPS) at 0.10 and 0.25 surfactin molar ratios (X_s) recorded on a subphase of 10 mM Tris, 150 mM NaCl at pH 7.2 and 20 °C. The surfactin curve is added on each graph to make easier its comparison with mixed surfactin–phospholipid curves.

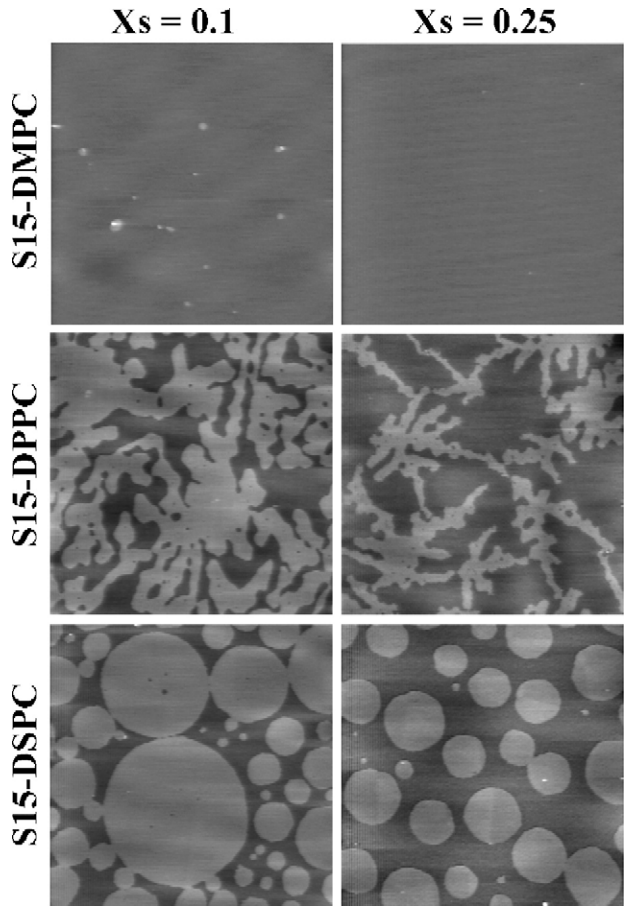

Fig. 3. AFM height images (5 μm×5 μm; z-scale: 3 nm) of mixed surfactin–phospholipid monolayers: S15-DMPC, S15-DPPC and S15-DSPC containing 10 mol% (X_s=0.1) or 25 mol% (X_s=0.25) of surfactin. The transfers on mica support were achieved at 20 mN/m.

phospholipid monolayers. For this reason, the domains observed in the images of the present study can be attributed to the effect of surfactin. Influence of PC acyl chains on domains structure has already been shown for other molecules like sphingomyelin (SM) [34]. These authors have shown that in mixed SM/unsaturated PC supported bilayers, SM-enriched gel domains can adopt a variety of morphologies in the fluid PC matrix, going from large flat homogeneous domains to branched filamentous aggregates. Some of these structures were dependent on the PC species (monounsaturated POPC or diunsaturated DOPC) present in the SM/PC mixtures. In our case, an almost homogeneous film is observed with DMPC while a phase separation is revealed in monolayers with DPPC and DSPC. For DPPC the higher domains (grey colour) are elongated and ramified while they have a rounded shape for DSPC. On the basis of previous studies [10,13], the lower matrix can be assigned to surfactin-enriched phase while higher domains would be mainly composed of phospholipids.

In the case of DMPC, the absence of domains, together with the absence of deviation from the additivity rule tend to suggest that surfactin is completely miscible to DMPC molecules. The absence of sharp deviation of mean molecular area excludes the formation of a complex between surfactin and DMPC as also evoked by Maget-Dana and Ptak [9]. Surfactin is probably distributed between the DMPC molecules perturbing the cooperative behaviour of phospholipid molecules. It is in accordance with the less favourable interaction energy between DMPC molecules in presence of surfactin, especially with S1 peptide cycle model (Fig. 4A and C). As already evoked by Eeman et al., the fluid-like state of DMPC monolayer is favourable to its miscibility with surfactin molecules [13].

In the case of DPPC and DSPC, AFM images reveal a clear phase separation (Fig. 3). The less favourable interaction energies of mixed assemblies compared to surfactin self-assemblies (Fig. 4B and C) show a low tendency of surfactin to be mixed with phospholipids, which is in accordance with

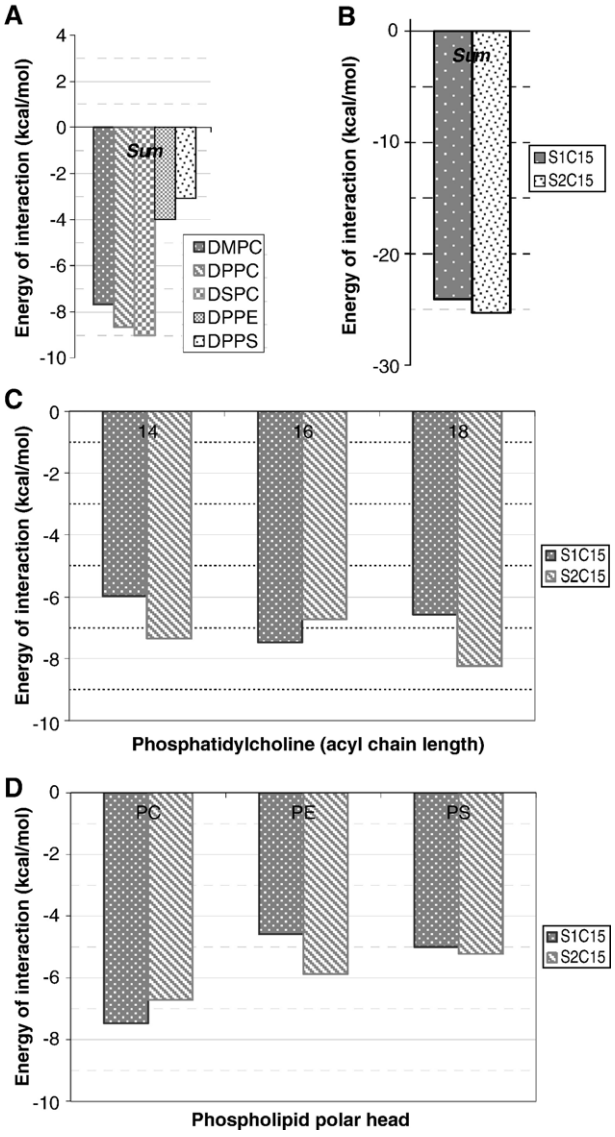

Fig. 4. Total energy of interaction of (A) pure phospholipids (DMPC, DPPC, DSPC, DPPE and DPPS); (B) pure surfactin with two peptide cycle configurations (S1 and S2); (C) mixed assemblies of surfactin with phospholipids differing by their alkyl chain length (DMPC, DPPC, DSPC); (D) mixed assemblies of surfactin with phospholipids differing by their polar head nature (DPPC, DPPE, DPPS).

results of Heerklotz and Seelig [35] showing the strong preference of surfactin for micelle formation over membrane insertion. This is in favour of an immiscibility of the two species. Moreover, the energy of interaction between lipid molecules is less favourable when surfactin is inserted into these lipids (Fig. 4A and C), which is also an argument for phase separation. The increasing mismatch between the hydrophobic length of surfactin and DPPC or DSPC monolayer thickness is probably at the origin of domains formation. The hydrophobic mismatch is known to play a key role in lipid–peptide organization [36–38]. Step height measured between the dark and the grey domains in AFM images (DPPC: 1.17 nm–DSPC: 1.34 nm) and distances between the ends of surfactin and phospholipid alkyl chains in models of mixed assemblies (Fig. 5B) give evidence of this discrepancy. This interfacial organization is also accentuated by the different physical state of surfactin and the two phospholipids. Both DPPC and DSPC are in a solid-like state while surfactin adopts a fluid-like state. These two opposite states promote the immiscibility between the two components at the interface.

The change in domain shape is likely to originate from a difference in the molecular interactions within the film. The domain size and shape result of a competition between two contradictory forces, namely the line tension, which works to reduce the interface of mismatch, and the long range dipole interactions, which act against the line tension at the boundary [39–42]. Circular shapes are favoured when the line tension of the interface between the two lipid phases dominates, while distorted, elongated structures are favoured when the electrostatic dipole–dipole repulsion between the molecular dipoles associated with the phospholipid molecules becomes dominant.

Compared to surfactin–DPPC system, surfactin–DSPC mixed monolayer exhibits a higher hydrophobic mismatch resulting in a higher value of the line tension component. As these two phospholipids differ only by the acyl chains length, repulsive electrostatic interactions are similar (0.25 and 0.21 kcal/mol for DPPC and DSPC, respectively). Consequently, for DSPC, the two opposite forces balance in favoured of circular domains formation while elongated and ramified structures observed with DPPC are governed by a lower line tension component. Such elongated and ramified DPPC domains floating on a surfactin-enriched phase were also observed for mixed surfactin–DPPC monolayers with a water subphase at pH 2.0 [10]. In the present study, addition of Na^+ ions in the subphase (NaCl 150 mM) has a shielding effect on the two partial negative charges borne by surfactin at pH 7.2, and consequently, gives rise to quite similar phase separation than the one observed at pH 2.0, when surfactin is protonated. This is in agreement with mixed surfactin–DPPC monolayer transferred from an aqueous subphase at pH 8.0 without NaCl. Indeed, the corresponding AFM image (Fig. 6) reveals also immiscibility between surfactin and DPPC but the lipid domains are more round and bigger than the ones observed at low pH. The change in domain shape/size is attributed to the presence of two negative charges on surfactin molecules at pH 8.0, which modify the conformation of the surfactin peptide cycle at the interface and, consequently, increase the immiscibility with DPPC [43]. Comparison of interfacial molecular

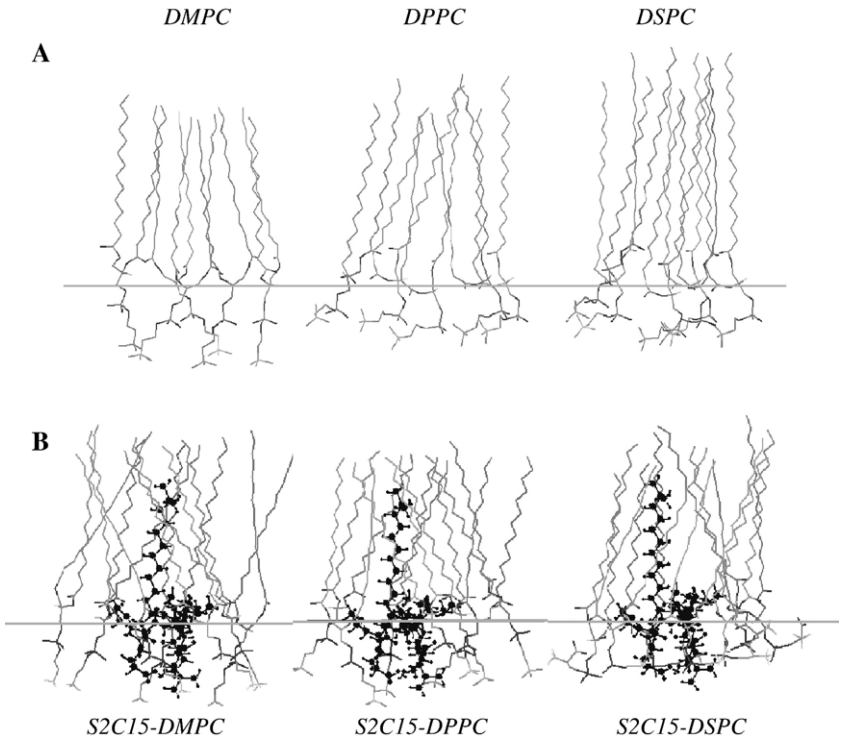

Fig. 5. (A) Self-assemblies of pure phospholipids: DMPC, DPPC and DSPC; (B) assembly of surfactin molecule with the peptide cycle configuration S2 (black sticks and balls) surrounded by phospholipids: DMPC, DPPC and DSPC.

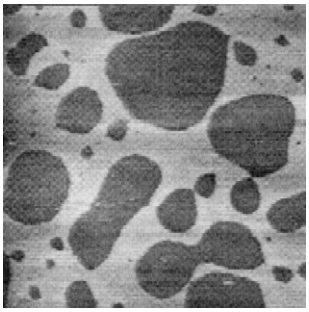

Fig. 6. AFM height image of mixed surfactin-DPPC containing 25 mol% (X_s=0.25) of surfactin. Subphase: Tris 5 mM pH 8.0. Temperature: 20 °C. Image size: 5 μm×5 μm. The transfers on mica support were achieved at 20 mN/m.

areas and AFM step height values emphasizes also the role of NaCl for partially screening the negative charges of surfactin. Indeed, in presence of sodium cations, these parameters are much closer to the ones obtained for protonated surfactin than the ones of the ionized molecule ($A_{20\ mN/m}$=142, 151 and 166 Å^2/ molecule and Δh=1.2, 1.17 and 0.8 nm with pH 2.0, pH 7.2/NaCl and pH 8.0 aqueous subphase, respectively).

The respect of the additivity rule suggests that surfactin and phospholipids (DPPC or DSPC) could be treated as non-interacting molecules, in other words that the mean molecular area of the lipids is not modified by the presence of the surfactin and vice-versa (data not shown). However, the surface coverage of lower domains in AFM images at 20 mN/m is higher (Table 1) than the surface percentage (S) occupied by surfactin in mixed monolayers at the air–water interface, calculated from Eq. (3) on basis of molecular areas taken from compression isotherms:

$$S = \lfloor X_s A_s / (X_s A_s + (1 - X_s) A_{PL}) \rfloor \times 100 \quad (3)$$

where X_s and A_s are the molar fraction and the mean molecular area of surfactin respectively and A_{PL} is the mean molecular area of phospholipid.

A hypothesis is that surfactin disturbs the packing of phospholipid molecules at the boundary between the two domains. In this case, the boundaries of the phospholipid domains are deformed to a greater extent by the AFM tip and cannot consequently be distinguished from surfactin domains. The reduction of the solid lipid domain size in monolayers by surfactants (like surfactant protein B and C) have already been observed [44,45]. Rinia et al. [46] have proposed a molecular model of DPPC bilayers in presence of incorporated model peptides showing clearly the disorder affecting the boundary of the phospholipid solid-like domains. As only a few parts of the phospholipid molecules are disturbed, the mean molecular area of the two components is globally not affected. The increasing discrepancy between the AFM coverage and the calculated one with surfactin molar fraction is in agreement with this hypothesis. Indeed, a larger proportion of surfactin in the mixed bidimensional system increases the contact perimeter between surfactin and phospholipid molecules, which is susceptible to be disturbed. Deformation of solid lipid domains by surrounding peptide molecules may also be related to the hydrophobic mismatch effect. Indeed experimental data (deuterium NMR [47] and electron cryomicroscopy [48] studies) have indicated a reduction in both acyl chain order and lipid layer thickness if an embedded peptide exhibits a smaller hydrophobic moiety than that of the lipid membrane model. Such adaptations for the relief of hydrophobic mismatch in mixed peptide–lipid membranes have to concern mainly molecules located at the boundaries of lipid domains, i.e. molecules just in contact with the peptide molecules, and probably explain the higher surfactin coverage observed in our AFM images. This hypothesis is in agreement with theoretical studies [36,38,49] which predict that perturbation in lipid thickness decreases for lipid molecules that are at a greater distance from incorporated peptide.

3.2. Effect of phospholipid polar head

At 20 mN/m, DPPE and DPPS have a molecular area of 42.1 and 47.4 Å^2 respectively (Fig. 2) which is in good agreement with other studies [50,51]. At this surface pressure, both pure phospholipids are in a solid-like state. The smaller volume of DPPE headgroup comparatively to DPPC and DPPS ones leads to a self-assembly with a cone shape as shown by modeling (Fig. 7A) and described in literature [52]. It explains its higher tight packing and consequently its smaller surface area observed in Π-A isotherm. The presence of strong intermolecular hydrogen bonding between PE headgroups contributes also considerably to the compacted interfacial organization of this lipid [25]. However, DPPE assembly is less stable than DPPC (Fig. 4A). The small size of PE polar heads leads to a proximity of the partial charges from the phosphate and ethanolamine moieties, which explains the higher value of the electrostatic repulsion comparatively with the PC polar heads (0.25 kcal/mol for DPPC versus 2.23 kcal/mol for DPPE). DPPS forms the most unfavourable assemblies (Fig. 4A). The presence of a negative net charge (like DPPS) perturbs the fatty acid chain organization. The net negative charge on the polar head is at the origin of the most positive and most unfavourable electrostatic interaction (2.63 kcal/mol).

Modifying the electrostatic properties or the volume of the phospholipid headgroup plays a significant role in modulating

Table 1
Surface percentage of lower domains observed in AFM images, and surface percentage of surfactin calculated from Eq. (3)

	X_s=0.1		X_s=0.25	
	AFM area (%)[a]	S (%) (Eq. (3))[b]	AFM area (%)[a]	S (%) (Eq. (3))[b]
DMPC	–	22	–	45.8
DPPC	36.6±4.5	25.8	73.4±6.3	51.1
DSPC	39.7±3.8	25.7	68.8±4.4	50.9
DPPE	36.8±3.7	28.5	69.2±5.4	54.4
DPPS	37.8±6.1	26.2	72.9± 3.5	51.5

[a] Surface percentage occupied by lower domains in AFM images.
[b] Surface occupied by surfactin in mixed surfactin–phospholipid monolayers at the air–water interface and calculated from Eq. (3).

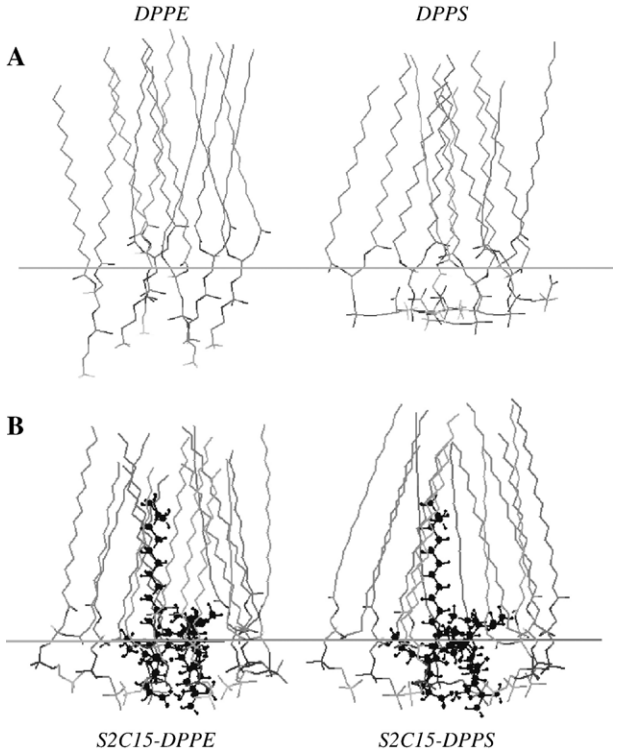

Fig. 7. (A) Self-assemblies of pure phospholipids: DPPE and DPPS; (B) Assembly of surfactin molecule with the peptide cycle configuration S2 (black sticks and balls) surrounded by phospholipids: DPPE and DPPS.

the mutual organization and interactions of surfactin with phospholipid molecules.

The absence of deviation from the additivity rule (data not shown) and the presence of distinct domains in AFM topographic images (Fig. 8) suggest in a first approach an immiscibility between surfactin and the three analyzed phospholipids, whatever the headgroup nature (PC, PE or PS). However, the shape of the lipid domains dramatically changes with the polar head nature. While elevated domains formed in the presence of DPPE and DPPS have a rounded shape and are interconnected, they are more extended and ramified with DPPC. In the case of DPPS, a higher surfactin molar fraction causes a separation of these domains which become more circular. These observations suggest that miscibility of surfactin with phospholipids occurs in the order DPPC > DPPE > DPPS.

AFM data correlate with the energy of interaction calculated for the mixed assembly models (Fig. 4D), which also shows a more likely association of surfactin with DPPC than with DPPE and DPPS. However, the energy of interaction of the mixed assembly surfactin–DPPE or surfactin–DPPS is more favourable than energy of the corresponding phospholipids self-assembly while it is less likely in the case of surfactin–DPPC (Fig. 4A and D). Surfactin is thus able to destabilize DPPC assembly while it stabilizes the interactions towards DPPE and DPPS molecules.

According to the models (Fig. 7A and B), insertion of surfactin between the polar headgroups of DPPE molecules takes away phospholipid molecules from each other. A geometrical accommodation between the two components would be at the origin of the stabilization. Indeed, the inverted-cone conformation of surfactin molecules tends to counter-balance the ability of the PE molecules to form hexagonal phases. It is in accordance with the study of Grau and co-workers [12] which have shown a stabilization effect of surfactin towards another PE phospholipid (DEPE) by differential scanning calorimetry measurements. The fact that both DPPE [53–55] and surfactin [56] are able to form inter- and intramolecular hydrogen bonding, respectively, can also contribute to this increasing stability of DPPE assemblies by incorporating surfactin molecules.

In the case of DPPS, stabilizing effect of surfactin can be explained by an additional shielding effect of electrostatic repulsions between the negative headgroup of DPPS molecules by the large surfactin peptide cycle rather by a geometrical accommodation. Indeed, insertion of surfactin molecules into the DPPS monolayers leads to a decrease of the electrostatic repulsions between the phospholipid molecules (2.63 kcal/mol for pure DPPS assembly versus 1.80 kcal/mol for surfactin–DPPS assembly). Moreover a strengthening of hydrophobic interactions between the components of the assembly (−4.90 kcal/mol for pure DPPS assembly versus −6.20 kcal/mol for surfactin–DPPS assembly) is observed by adding

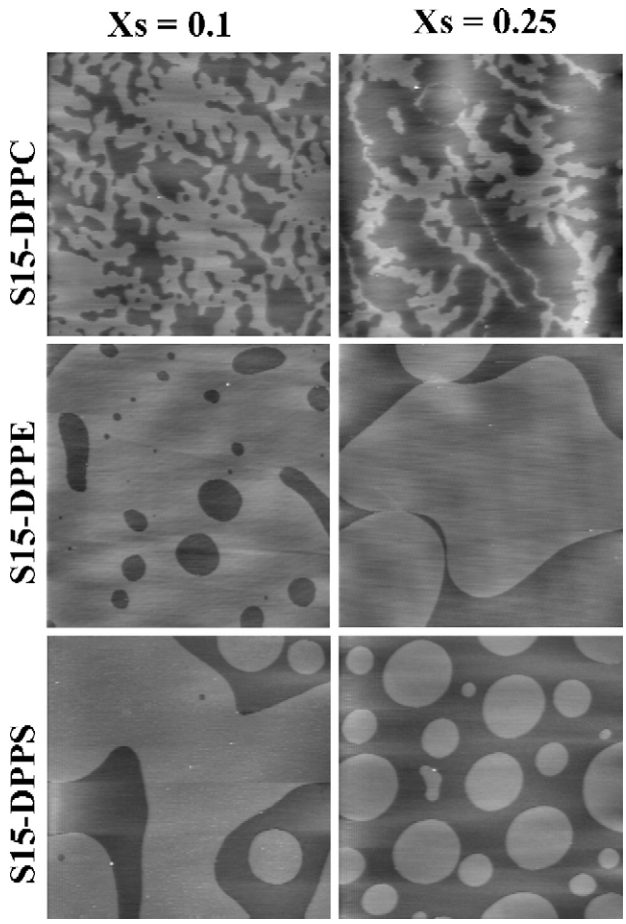

Fig. 8. AFM height images (5 μm × 5 μm; z-scale: 3 nm) of mixed surfactin–phospholipid monolayers : S15-DPPC, S15-DPPE and S15-DPPS containing 10 mol% (X_s = 0.1) or 25 mol% (X_s = 0.25) of surfactin. The transfers on mica support were achieved at 20 mN/m.

surfactin. This higher hydrophobic interaction tends to favour a cone-shape arrangement of the mixed assembly (Fig. 7B).

The surface coverage of lower domains in AFM is higher than the percentage calculated for surfactin from Eq. (3). As evoked above, it suggests that surfactin disturbs the boundaries of the phospholipid domains without affecting the mean molecular area of the two components as the additivity rule is respected (data not shown).

4. Conclusion and summary

This study shows that AFM, in combination with the molecular modeling and the surface pressure-area isotherms, is a powerful approach to probe the molecular organization of lipopeptide–phospholipid monolayers at a nanoscale resolution. The interactions between surfactin and phospholipids, and their mutual organization at an interface dramatically depend on both the chain length (14, 16 and 18 carbon atoms) and the polar head of phospholipid (large and zwitterionic PC, small and zwitterionic PE, negatively charged PS).

Comparatively to studies of Maget-Dana and Ptak [9] and Grau et al. [12], our work further analyzes the miscibility between surfactin and phospholipids differing by their acyl chain length or by their polar head. The transfer surface pressure of mixed surfactin–phospholipid monolayers for AFM imaging is fixed at 20 mN/m in order to additionally investigate the effect of the phospholipid physical state, as we have shown in a previous study [13] the importance of this parameter on the interfacial behaviour of surfactin.

While Grau et al. have suggested specific molecular interactions between DMPC acyl chains and surfactin [12], our results highlight an ideal miscibility, i.e. an interfacial arrangement of the two components without mutual influence. They are in complete agreement with Maget-Dana and Ptak study [9]. The difference between Grau et al. results and ours might arise from the model system used, and more particularly, from the lateral pressure inside the model. Whereas they have dealt with bilayer models where the lateral pressure is probably higher than 30 mN/m [57], we use monolayer systems at 20 mN/m.

Moreover, our work emphasizes miscibility discrepancy when surfactin is mixed with DPPC or DSPC while Grau et al. [12] have not observed any significant difference. In our study, considering the domains shapes observed in AFM images, the miscibility between surfactin and phospholipids decreases with increasing phospholipid chain length. The physical state (fluid-like or solid-like) adopted by the phospholipids in the mixed monolayers and the hydrophobic mismatch between the two components are the two main parameters driving the arrangement of the molecules at the interface. Thus, surfactin perturbs more strongly membranes containing phospholipids which have shorter chain length and/or which are in a fluid-like organization. By this effect, surfactin would also be able to insert into the boundary of membrane rafts, which have been shown to have a more disordered organization [58], and consequently have an influence on their biological functions.

The polar headgroup of phospholipids is known to have an influence on the interfacial behaviour of surfactin. Our results explicitly show the stabilizing effect of surfactin towards DPPE monolayer, which confirms the hypothesis of Grau et al. [12]. Molecular modeling clearly displays that this effect can be attributed to a geometrical accommodation between surfactin and DPPE molecules. The surfactin ability to modify the geometry of monolayer including PE can be related to its antiviral activity [Deleu, M., unpublished data] [6,59]. The presence of surfactin impairs probably the ability of PE to undergo transition from bilayer to inverted hexagonal structure, which is known to catalyze the fusion process between virus and host cell membrane [60,61].

In addition to Grau et al. study [12], we also highlight the stabilizing effect of surfactin towards DPPS monolayer. In this case, a shielding effect of electrostatic repulsions between DPPS molecules as well as a strengthening of hydrophobic interactions between acyl chains of both phospholipid and surfactin are suggested to be at the origin of the phenomenon.

Furthermore, AFM images indicate that the polar headgroup of phospholipids influences the miscibility of surfactin in the order DPPC > DPPE > DPPS.

Results are also interesting for the design of efficient surfactin delivery systems. Playing on the balance between PC, PE and PS phospholipids in a liposome formulation should lead to an optimal delivery of surfactin into different kinds of target cells.

Acknowledgements

Y.F.D. and M.D. are Research Associates of the National Foundation for Scientific Research (F.N.R.S.) from Belgium. R.B. is Director of Research of F.N.R.S. The support of the Région wallonne (#021/5103) and of the F.N.R.S. is gratefully acknowledged.

The authors are thankful to P. Thonart and his team (Unité de Bio-industries, Faculté Universitaire des Sciences agronomiques de Gembloux, Belgium) for the production of the surfactin by fermentation of the *Bacillus subtilis* strain S499 and to E. Gaigneaux for the use of the atomic force microscope.

References

[1] K. Arima, A. Kakinuma, G. Tamura, Surfactin, a crystalline peptide–lipid surfactant produced by *B. subtilis*: isolation, characterization and its inhibition of fibrin clot formation, Biochem. Biophys. Res. Commun. 31 (1968) 488–494.

[2] A. Kakinuma, A. Ouchida, T. Shima, H. Sugino, M. Isono, G. Tamura, K. Arima, Confirmation of the structure of surfactin by mass spectrometry, Agric. Biol. Chem. 33 (1969) 1669–1671.

[3] Y. Kameda, S. Oira, K. Matsui, S. Kanatomo, T. Hase, Antitumor activity of *Bacillus natto*. V. Isolation and characterization of surfactin in the culture medium of *Bacillus natto* KMD 2311, Chem. Pharm. Bull. 22 (1974) 938–944.

[4] A.W. Bernheimer, L.S. Avigad, Nature and properties of a cytolytic agent produced by *Bacillus subtilis*, J. Gen. Microbiol. 61 (1970) 361–369.

[5] K. Hosono, H. Suzuki, Acylpeptides, the inhibitors of cyclic adenosine 3′, 5′-monophosphate phosphodiesterase. I. Purification, physicochemical properties and structures of fatty acid residues, J. Antibiot. 36 (1983) 667–673.

[6] D. Vollenbroich, M. Özel, J. Vater, R.M. Kamp, G. Pauli, Mechanism of inactivation of enveloped viruses by the biosurfactant surfactin from *Bacillus subtilis*, Biologicals 25 (1997) 289–297.
[7] D. Vollenbroich, G. Pauli, M. Özel, J. Vater, Antimycoplasma properties and application in cell culture of surfactin, a lipopeptide antibiotic from *Bacillus subtilis*, Appl. Environ. Microbiol. 63 (1997) 44–49.
[8] J.D. Sheppard, C. Jumarie, D.G. Cooper, R. Laprade, Ionic channels induced by surfactin in planar lipid bilayer membranes, Biochim. Biophys. Acta 1064 (1991) 13–23.
[9] R. Maget-Dana, M. Ptak, Interactions of surfactin with membrane models, Biophys. J. 68 (1995) 1937–1943.
[10] M. Deleu, M. Paquot, P. Jacques, P. Thonart, Y. Adriaensen, Y.F. Dufrêne, Nanometer scale organization of mixed surfactin/phosphatidylcholine monolayers, Biophys. J. 77 (1999) 2304–2310.
[11] M. Deleu, K. Nott, R. Brasseur, P. Jacques, P. Thonart, Y.F. Dufrêne, Imaging mixed lipid monolayers by dynamic atomic force microscopy, Biochim. Biophys. Acta 1513 (2001) 55–62.
[12] A. Grau, J.C. Gómez Fernández, F. Peypoux, A. Ortiz, A study on the interactions of surfactin with phospholipid vesicles, Biochim. Biophys. Acta 1418 (1999) 307–319.
[13] M. Eeman, A. Berquand, Y.F. Dufrêne, M. Paquot, S. Dufour, M. Deleu, Penetration of surfactin into phospholipid monolayers: nanoscale interfacial organization, Langmuir 22 (2006) 11337–11345.
[14] Y.F. Dufrêne, W.R. Barger, J.-B.D. Green, G.U. Lee, Nanometer-scale surface properties of mixed phospholipid monolayers and bilayers, Langmuir 13 (1997) 4779–4784.
[15] S.D. Connell, D.A. Smith, The atomic force microscopy as a tool for studying phase separation in lipid membranes, Mol. Membr. Biol. 23 (2006) 17–28.
[16] R. Maget-Dana, The monolayer technique: a potent tool for studying the interfacial properties of antimicrobial and membrane-lytic peptides and their interactions with lipid membranes, Biochim. Biophys. Acta 1462 (1999) 109–140.
[17] M. Deleu, M. Paquot, T. Nylander, Fengycin interaction with lipid monolayers at the air-aqueous interface- implications for the effect of fengycin on biological membranes, J. Colloid Interface Sci. 283 (2005) 358–365.
[18] M. Eeman, M. Deleu, M. Paquot, P. Thonart, Y. Dufrene, Nanoscale properties of mixed fengycin/ceramide monolayers explored using atomic force microscopy, Langmuir 21 (2005) 2505–2511.
[19] L. Lins, P. Ducarme, E. Breukink, R. Brasseur, Computational study of nisin interaction with model membrane, Biochim. Biophys. Acta 1420 (1999) 111–120.
[20] M. Deleu, O. Bouffioux, H. Razafindralambo, M. Paquot, C. Hbid, P. Thonart, P. Jacques, R. Brasseur, Interaction of surfactin with membranes: a computational approach, Langmuir 19 (2003) 3377–3385.
[21] X. Gallet, M. Deleu, H. Razafindralambo, P. Jacques, P. Thonart, M. Paquot, R. Brasseur, Computer simulation of surfactin conformation at a hydrophobic/hydrophilic interface, Langmuir 15 (1999) 2409–2413.
[22] J.-M. Bonmatin, M. Genest, H. Labbé, M. Ptak, Solution three-dimensional structure of surfactin: a cyclic lipopeptide studied by ^{1}H-NMR, distance geometry, and molecular dynamics, Biopolymers 34 (1994) 975–986.
[23] R. Brasseur, E. Goormaghtigh, J.-M. Ruysschaert, Theoretical conformational analysis of phospholipids bilayers, Biochem. Biophys. Res. Commun. 103 (1981) 301–310.
[24] G. Bult, H.U. Gally, A. Seelig, G. Zaccai, Neutron diffraction studies on selectively deuterated phospholipids bilayers, Nature 271 (1978) 182–184.
[25] M. Dyck, P. Krüger, M. Lösche, Headgroup organization and hydration of methylated phosphatidylethanolamines in Langmuir monolayers, Phys. Chem. Chem. Phys. 7 (2005) 150–156.
[26] R. Brasseur, TAMMO : Theoretical Analysis of Membrane Molecular Organization, in: R. Brasseur (Ed.), Molecular Description of Biological Membranes by Computer Aided Conformational Analysis, CRC Press, Boca Raton, FL, 1990, pp. 203–219.
[27] R. Brasseur, M. Deleers, J.-M. Ruysschaert, Mode of organization of amphiphilic molecules at a lipid–water interface: a conformational analysis, J. Colloid Interface Sci. 114 (1986) 277–281.
[28] R. Brasseur, M. Deleers, J.-M. Ruysschaert, Sequence of ionophore conformational changes induced by a simulated membrane/water interface, Biosci. Rep. 4 (1984) 651–658.
[29] H. Razafindralambo, M. Paquot, C. Hbid, P. Jacques, P. Thonart, Purification of antifungal lipopeptides by reversed-phase high-performance liquid chromatography, J. Chromatogr. 639 (1993) 81–85.
[30] M.C. Philipps, D. Chapman, Monolayer characteristics of saturated 1,2-diacylphosphatidylcholines (lecithins) and phosphatidylethanolamines at the air–water interface, Biochim. Biophys. Acta 163 (1968) 301–313.
[31] V.L. Shapovalov, E.A. Kotova, T.I. Rokitskaya, Y.N. Antonenko, Effect of gramicidin A on the dipole potential of phospholipid membranes, Biophys. J. 77 (1999) 299–305.
[32] F. Bordi, C. Cametti, F. De Luca, T. Gili, D. Gaudino, S. Sennato, Charged lipid monolayers at the air-solution interface: coupling to polyelectrolytes, Colloids Surf., B Biointerfaces 29 (2003) 149–157.
[33] L. Zhao, S. Feng, Effects of lipid chain length on molecular interactions between paclitaxel and phospholipid within model biomembranes, J. Colloid Interface Sci. 74 (2004) 55–68.
[34] M. Giocondi, V. Vie, E. Lesniewska, P. Milhiet, M. Zinke-Allmang, C. Le Grimellec, Phase topology and growth of single domains in lipid bilayers, Langmuir 17 (2001) 1653–1659.
[35] H. Heerklotz, J. Seelig, Detergent-like action of the antibiotic peptide surfactin on lipid membranes, Biophys. J. 81 (2001) 1547–1554.
[36] D. Fattal, A. Benshaul, A molecular-model for lipid–protein interaction in membranes — the role of hydrogen mismatch, Biophys. J. 65 (1993) 1795–1809.
[37] J.A. Killian, Hydrophobic mismatch between proteins and lipids in membranes, Biochim. Biophys. Acta 1376 (1998) 401–416.
[38] E. Wallace, N. Hooper, P. Olmstedz, Effect of hydrophobic mismatch on phase behavior of lipid membranes, Biophys. J. 90 (2006) 4104–4118.
[39] R.D. De Koker, H.M. McConnell, Circle to dogbone: shapes and shape transitions of lipid monolayer domains, J. Phys. Chem. 97 (1993) 13419.
[40] M. Seul, D. Andelman, Domain shapes and patterns — the phenomenology of modulated phases, Science 267 (1995) 476–483.
[41] S. Perkovic, H. McConnell, Cloverleaf monolayer domains, J. Phys. Chem., B 101 (1997) 381–388.
[42] V. Smorodin, E. Melo, Shape and dimensions of gel-domains in phospholipid bilayers: a theoretical study, J. Phys. Chem., B 105 (2001) 6010–6016.
[43] M. Deleu, Propriétés de la surfactine et de la fengycine A aux interfaces liquide/liquide et dans des emulsions modèles, PhD thesis, Gembloux Agricultural University, 2000, 236p.
[44] M. Amrein, A. vonNahmen, M. Sieber, A scanning force and fluorescence light microscopy study of the structure and function of a model pulmonary surfactant, Eur. Biophys. J. 26 (1997) 349–357.
[45] S. Krol, M. Ross, M. Sieber, S. Kunneke, H. Galla, A. Janshoff, Formation of three-dimensional protein–lipid aggregates in monolayer films induced by surfactant protein B, Biophys. J. 79 (2000) 904–918.
[46] H. Rinia, J. Boots, D. Rijkers, R. Kik, M. Snel, R. Demel, J. Killian, J. van der Eerden, B. de Kruijff, Domain formation in phosphatidylcholine bilayers containing transmembrane peptides: specific effects of flanking residues, Biochemistry 41 (2002) 2814–2824.
[47] M. de Planque, D. Greathouse, R. Koeppe, H. Schafer, D. Marsh, J. Killian, Influence of lipid/peptide hydrophobic mismatch on the thickness of diacylphosphatidylcholine bilayers. A H-2 NMR and ESR study using designed transmembrane alpha-helical peptides and gramicidin A, Biochemistry 37 (1998) 9333–9345.
[48] Y. Tahara, M. Murata, S. Ohnishi, Y. Fujiyoshi, M. Kikuchi, Y. Yamamoto, Functional signal peptide reduces bilayer thickness of phosphatidylcholine liposomes, Biochemistry 31 (1992) 8747–8754.
[49] D. Duque, X. Li, K. Katsov, M. Schick, Molecular theory of hydrophobic mismatch between lipids and peptides, J. Chem. Phys. 116 (2002) 10478–10484.
[50] J. Miñones, J.M.R. Patino, O. Conde, C. Carrera, R. Seoane, The effect of polar groups on structural characteristics of phospholipid monolayers spread at the air–water interface, Colloids Surf., A Physicochem. Eng. Asp. 203 (2002) 273–286.

[51] L. Zhao, S.-S. Feng, Effects of lipid chain unsaturation and headgroup type on molecular interactions between paclitaxel and phospholipids within model biomembrane, J. Colloid Interface Sci. 285 (2005) 326–335.
[52] L. Chernomordik, Non-bilayer lipids and biological fusion intermediates, Chem. Phys. Lipids 81 (1996) 203–213.
[53] A. Sen, P. Yang, H. Mantsch, S. Hui, Extended hydrogen-bonded structures of phosphatidylethanolamine, Chem. Phys. Lipids 47 (1988) 109–116.
[54] J. Seddon, Structure of the inverted hexagonal (HII) phase, and non-lamellar phase-transitions of lipids, Biochim. Biophys. Acta 1031 (1990) 1–69.
[55] D. Pink, S. McNeil, B. Quinn, M. Zuckermann, A model of hydrogen bond formation in phosphatidylethanolamine bilayers, Biochim. Biophys. Acta, Biomembr. 1368 (1998) 289–305.
[56] J.P. Nicolas, Molecular dynamics simulation of surfactin molecules at the water–hexane interface, Biophys. J. 85 (2003) 1377–1391.
[57] D. Marsh, Lateral pressure in membranes, Biochim. Biophys. Acta 1286 (1996) 183–223.
[58] P. Kuzmin, S. Akimov, Y. Chizmadzhev, J. Zimmerberg, F. Cohen, Line tension and interaction energies of membrane rafts calculated from lipid splay and tilt, Biophys. J. 88 (2005) 1120–1133.
[59] M. Kracht, H. Rokos, M. Ozel, M. Kowall, G. Pauli, J. Vater, Antiviral and hemolytic activities of surfactin isoforms and their methyl ester derivatives, J. Antibiot. 52 (1999) 613–619.
[60] P.R. Cullis, D.B. Fenske, M.J. Hope, in: D.E. Vance, J. Vance (Eds.), New Comprehensive Biochemistry, Biochemistry of Lipids, Lipoproteins and Membranes, vol. 31, Elsevier, North-Holland, Amsterdam, 1996, pp. 1–33.
[61] H. Itokawa, T. Miyashita, H. Morita, K. Takeya, T. Hirano, M. Homma, K. Oka, Structural and conformational studies of [Ile7] and [Leu7]surfactins from *Bacillus subtilis natto*, Chem. Pharm. Bull. 42 (1994) 604–607.